Tailored anomalous group-velocity dispersion in silicon channel waveguides

Amy C. Turner, Christina Manolatou, Bradley S. Schmidt, and Michal Lipson

School of Electrical and Computer Engineering, Cornell University, Ithaca, NY 14853
lipson@ece.cornell.edu

Mark A. Foster, Jay E. Sharping, and Alexander L. Gaeta

School of Applied and Engineering Physics, Cornell University, Ithaca, NY 14853

Abstract: We present the first experimental demonstration of anomalous group-velocity dispersion (GVD) in silicon waveguides across the telecommunication bands. We show that the GVD in such waveguides can be tuned from -2000 to 1000 ps/(nm·km) by tailoring the cross-sectional size and shape of the waveguide.

OCIS codes: (130.2790) Guided waves; (230.7380) Waveguides, channeled; (060.5530) Pulse propagation and solitons.

References and links

1. M. A. Foster, K. D. Moll, and A. L. Gaeta, "Optimal waveguide dimensions for nonlinear interactions," Opt. Express **12**, 2880-2887 (2004).
2. V. R. Almeida, C. A. Barrios, R. R. Panepucci, and M. Lipson, "All-optical control of light on a silicon chip," Nature **481**, 1081-1084 (2004).
3. R. Claps, D. Dimitropoulos, V. Raghunathan, Y. Han, and B. Jalali, "Observation of stimulated Raman amplification in silicon waveguides," Opt. Express **11**, 1731-1739 (2003).
4. Y. A. Vlasov, M. O'Boyle, H. F. Hamann, and S. J. McNab, "Active control of slow light on a chip with photonic crystal waveguides," Nature **438**, 65-69 (2005).
5. M. J. Weber, "Silicon (Si)" and "Fused silica (SiO2)" in *Handbook of optical materials*, (CRC Press, Boca Raton, 2003).
6. L. Tong, J. Lou, and E. Mazur, "Single-mode guiding properties of subwavelength-diameter silica and silicon wire waveguides," Opt. Express **12**, 1025-1035 (2004).
7. V Raghunathan, R. Claps, D. Dimitropoulos, and B. Jalali, "Parametric Raman wavelength conversion in scaled silicon waveguides," J. Lightwave Technol. **23**, 2094-2102 (2005).
8. X. Chen, N. C. Panoiu, and R. M. Osgood, Jr., "Theory of Raman-mediated pulsed amplification in silicon-wire waveguides," IEEE J. Quantum Electron. **42**, 160-170 (2006).
9. G. P. Agrawal, *Fiber-Optic Communication Systems* (John Wiley & Sons, Inc., 1997).
10. L. F. Mollenauer, R. H. Stolen, and J. P. Gorden, "Experimental observation of picosecond pulse narrowing and solitons in optical fibers," Phys. Rev. Lett. **45**, 1095-1098 (1980).
11. G. P. Agrawal, *Nonlinear Fiber Optics* (Academic Press, 1989).
12. D. G. Ouzounov, D. Homoelle, W. Zipfel, W. W. Webb, A. L. Gaeta, J. A. West, J. C. Fajurdo, and K. W. Koch, "Dispersion measurements of microstructured fibers using femtosecond laser pulses," Opt. Commun. **192**, 219-223 (2001).
13. J. C. Knight, J. Arriaga, T. A. Birks, A. Ortigosa-Blanch, W. J. Wadsworth, and P. St. J. Russell, "Anomalous dispersion in photonic crystal fiber," IEEE Photon. Technol. Lett. **12**, 807-809 (2000).
14. J. E. Sharping, M. Fiorentino, A. Coker, P. Kumar, and R. S. Windeler, "Four-wave mixing in microstructure fiber," Opt. Lett. **26**, 1048 (2001).
15. W. H. Reeves, D. V. Skryabin, F. Biancalana, J. C. Knight, P. St. J. Russell, F. G. Omenetto, A. Efimov, and A. J. Taylor, "Transformation and control of ultra-short pulses in dispersion-engineered photonic crystal fibres," Nature **424,** 511-515 (2003).
16. J. E. Sharping, M. Fiorentino, P. Kumar, and R. S. Windeler, "Optical parametric oscillator based on four-wave mixing in microstructure fiber," Opt. Lett. **27** 1675-1677 (2002).
17. M. A. Foster, A. L. Gaeta, Q. Cao, and R. Trebino, "Soliton-effect compression of supercontinuum to few-cycle durations in photonic nanowires," Opt. Express **13** 6848-6855 (2005).
18. J. K. Ranka, R. S. Windeler, and A. J. Stentz, "Visible continuum generation in air-silica microstructure optical fibers with anomalous dispersion at 800 nm," Opt. Lett. **25**, 25-27 (2000).

#68155 - $15.00 USD Received 17 February 2006; revised 28 April 2006; accepted 1 May 2006

19. H. K. Tsang, C. S. Wong, T. K. Liang, I. E. Day, S. W. Roberts, A. Harpin, J. Drake, and M. Asghari, "Optical dispersion, two-photon absorption and self-phase modulation in silicon waveguides at 1.5 μm wavelength," Appl. Phys. Lett. **80**, 416-418 (2002).
20. H. Fukada, K. Yamada, T. Shoji, M. Takahashi, T. Tsuchizawa, T. Watanabe, J. Takahashi, and S. Itabashi, "Four-wave mixing in silicon wire waveguides," Opt. Express **13**, 4629-4637 (2005).
21. R. L. Espinola, J. I. Dadap, R. M. Osgood Jr., S. J. McNab, and Y. A. Vlasov, "C-band wavelength conversion in silicon photonic wire waveguides," Opt. Express **13**, 4341-4349 (2005).
22. V. R. Almeida, R. R. Panepucci, and M. Lipson, "Nanotaper for compact mode conversion," Opt. Lett. **28**, 1302-1304 (2003).
23. M. A. Foster, A. C. Turner, J. E. Sharping, B. S. Schmidt, M. Lipson, and A. L. Gaeta, "Broad-band optical parametric gain on a silicon photonic chip," submitted for publication (2006).

1. Introduction

Development of silicon-based nanophotonic devices for creating photonics-on-chip technology has recently been the subject of substantial research activity. The silicon-on-insulator (SOI) platform has inherent advantages for all-optical devices due to the high-index contrast between the silicon core and silica cladding, allowing for strong optical confinement and large effective nonlinearities [1]. Recently such waveguides have been analyzed for applications such as switching, amplification and slowing light [2–4]. For these and other applications control of the group-velocity dispersion (GVD) D of the waveguide is important. At the telecommunications wavelength of 1.55 μm, the material dispersion of crystalline silicon is large and normal [D = -880 ps/(nm·km) [5]]. Due to the high modal confinement in SOI waveguides, the waveguide dispersion can counteract the effect of the normal material dispersion and allow the waveguide to operate in an anomalous-GVD regime [6–8]. Controlling the effective dispersion in communication systems is critical for a number of applications. For example, dispersion compensation schemes that minimize the effects of temporal broadening of signal pulses are an essential component of current and future telecommunication systems [9]. Tailoring the dispersion is also crucial for increasing the effectiveness of numerous nonlinear optical processes such as soliton generation [10], soliton-effect pulse compression, and four-wave mixing [11]. As demonstrated with microstructured optical fibers [12, 13], careful control of the core diameter and the air-filling fraction of the cladding structure allows for tailored anomalous-GVD which has led to enhancement of numerous nonlinear optical processes such as four-wave mixing [14], Raman self-frequency shifting [15], parametric oscillation [16], extreme pulse self compression [17], and the widely-studied area of super-continuum generation [18].

In this paper we determine the waveguide geometries that allow for anomalous-GVD and investigate through numerical simulations how the waveguide cross-sectional shape and size can be used to control the resulting GVD. In agreement with our simulations, we measure experimentally that the GVD in silicon waveguides can be highly anomalous over a large bandwidth. We engineer the waveguide dimensions and experimentally measure normal- and anomalous-GVD ranging from -300 to 1100 ps/(nm·km) in the wavelength range of 1.35 to 1.55 μm. Specifically, at the telecommunications wavelength of 1.55 μm we tailor and experimentally verify the GVD to be in the range of anomalous values from 200 to 1100 ps/(nm·km) for four different sized waveguides. Careful choice of the waveguide shape and size is required to obtain anomalous-GVD at a desired wavelength.

#68155 - $15.00 USD Received 17 February 2006; revised 28 April 2006; accepted 1 May 2006

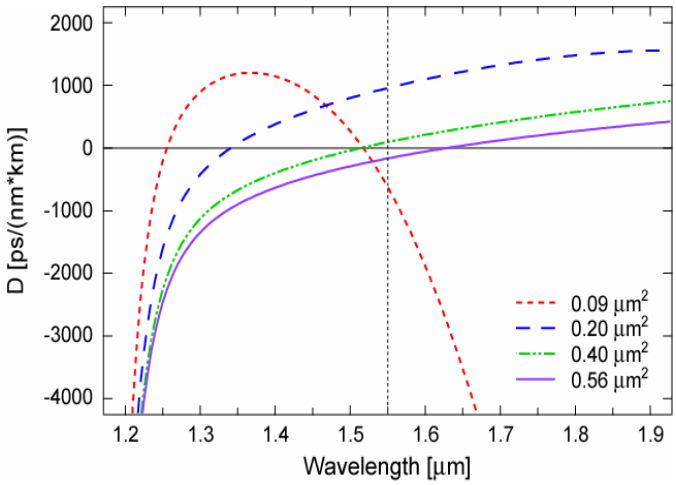

Fig. 1. Group-velocity dispersion *D* as a function of wavelength for a fixed aspect ratio of 1:1.5 (height to width) and for cross-sectional areas of 0.09 μm^2, 0.20 μm^2, 0.40 μm^2, and 0.56 μm^2.

2. Analysis

The tailoring of the GVD is enabled by controlling the degree of light confinement of the waveguide. This can be seen in Figs. 1 and 2 where we plot the GVD for the low-loss TE-like mode as numerically calculated for different cross-sectional areas and shapes using a custom, full-vector, finite-difference mode solver. Sellmeier equations representing pure crystalline silicon and fused silica [5] provide the input for the material dispersion of the core and cladding of the waveguide.

Figure 1 shows the plots of the GVD as the total cross sectional area is increased for a fixed aspect ratio of 1:1.5. Varying the cross-sectional area from 0.09 μm^2 to 0.56 μm^2 causes a significant change in the GVD. For the smallest waveguide, two zero-GVD points are within the wavelength range of interest whereas for the larger waveguide only one is present. Furthermore, the peak anomalous-GVD shifts from 1.35 to larger than 1.90 μm. From this plot it is clear that a careful choice of the waveguide size is necessary to achieve anomalous-GVD. For example, at a wavelength of 1.55 μm the smallest and largest waveguides shown in the figure yield normal-GVD, whereas, for the intermediate sizes anomalous-GVD is predicted. Previous experimental studies of the GVD of silicon waveguides were performed on a large waveguide with an area ~6 μm^2 and therefore resulted in a value corresponding to normal-GVD [19].

The aspect ratio of the waveguide also affects the dispersion, especially for highly confining waveguides. This can be seen in Figs. 2(a) and 2(b) where the GVD is plotted for waveguides with cross-sectional areas of 0.09 μm^2 and 0.56 μm^2, respectively. Figure 2(a) shows the geometric dependence of a single mode waveguide with cross-sectional area of 0.09 μm^2 for different aspect ratios. One can see that at a wavelength of 1.55 μm, the maximum possible GVD for rectangular waveguide areas of 0.09 μm^2 (see the green dashed curve corresponding to 212 nm x 425 nm) is still normal [-160 ps/(nm·km)]. This explains why, for example, the four-wave mixing efficiency previously observed in silicon was relatively low [20, 21]. For a 1:1 aspect ratio 300 nm x 300 nm (the red dashed curve in Fig. 2), the peak anomalous-GVD value is 1856 ps/(nm·km) at a wavelength of 1.35 μm.

For larger waveguides, the effect of the shape of the waveguide on the GVD is significantly decreased, and achieving anomalous-GVD in such waveguides in the 1.55 μm region is not assured. This can be seen in Fig. 2(b) where the simulations are repeated for a larger waveguide with a cross-sectional area of 0.56 μm^2. The GVD for this larger waveguide is weakly dependent on shape, which is a result of the weak modal confinement.

#68155 - $15.00 USD Received 17 February 2006; revised 28 April 2006; accepted 1 May 2006

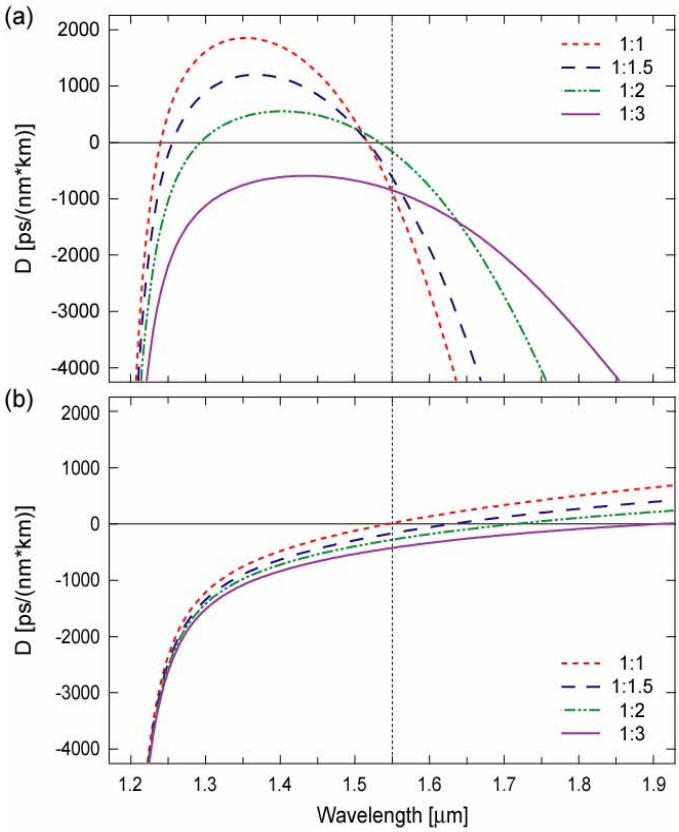

Fig. 2. Group-velocity dispersion as a function of wavelength for varying aspect ratios and fixed cross sectional areas of (a) 0.09 μm^2 and (b) 0.56 μm^2.

3. Fabrication

In order to analyze experimentally the tailoring of the GVD by varying the size and geometry, we fabricate four waveguides with a fixed height of 300 nm and create widths of different sizes using electron-beam lithography on an SOI platform with 1-μm buried oxide. The cross-sectional area for such waveguides is on the order of 0.20 μm^2 which corresponds to anomalous-GVD for the fundamental TE-like mode (see Fig. 1) near the 1.55 μm region. Each end of the waveguide is terminated with an inverse taper [22] in order to ensure that only the fundamental mode is excited. The 6.4-mm-long silicon waveguides are designed to have no bends in them so as to maintain propagation of the fundamental mode. The waveguides are etched using reactive-ion etching and clad with silica using plasma-enhanced chemical vapor deposition (PECVD). The measured propagation losses in the waveguides range from 1.1 to 1.4 dB/cm.

4. Experiment

In order to measure the GVD of the waveguides, we use Fourier-transform spectral interferometry (FTSI) to determine the group index as a function of wavelength for the four waveguides similar to the technique seen in Ref. 19. A picosecond laser pulse train from a tunable optical parametric oscillator is split such that one part is sent to the waveguide and the other travels through a reference arm. The waveguide branch is coupled using a laser-polished lens fiber. The polarization is optimized to excite the low-loss TE-like mode of the waveguide. The waveguide output is collected with a lens, sent through a polarizer to ensure the analysis of only the fundamental TE-like mode, and coupled back into a fiber. This signal

#68155 - $15.00 USD Received 17 February 2006; revised 28 April 2006; accepted 1 May 2006

is combined with the reference arm in a 90:10 coupler. When the output pulses are measured with an OSA one observes a wavelength-dependent modulation of the optical spectrum, or a spectral interferogram. The frequency of the modulation of the spectral interferogram is proportional to the time delay between the two pulses. By extracting the variation of the time delay as a function of the center wavelength of the pulses, one obtains the group index of refraction of the entire system. In order to find the group index solely of the waveguides, the measurements are repeated with the waveguide removed from the system. Although the measured waveguides are multimode, a very small fraction of the power is coupled into higher order modes. However, due to the extreme sensitivity of this spectral measurement technique, the signals due to these higher-order modes are easily differentiated, allowing for characterization of only the fundamental mode.

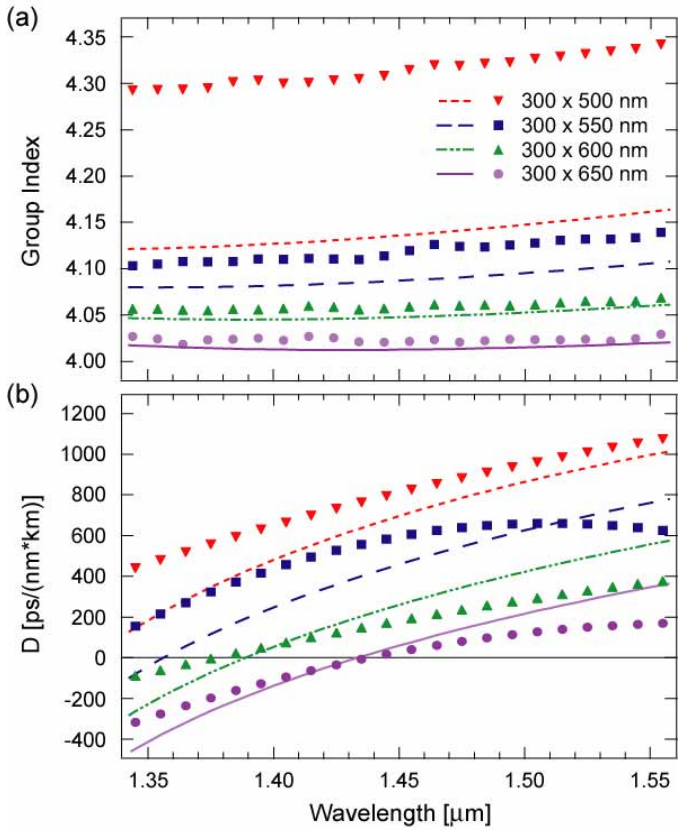

Fig. 3. Simulated (lines) and experimental (symbols) (a) group index data and (b) group-velocity dispersion as a function of wavelength for four different waveguides. Ellipsometric measurements are done on the PECVD over-cladding and then fitted with a Sellmeier function to provide the upper-cladding material dispersion data for the simulated curves.

By tuning the wavelength of the input pulse and repeating this procedure based on FTSI, we are able to obtain the group index as a function of wavelength (Fig 3a). For the waveguides studied here, the group index increases as a function of wavelength for most of the range which is indicative of anomalous-GVD. The group delay was measured 5 times at each wavelength and the results were averaged. This produced a 0.1% error in the measurement of group index. This error does not include inaccuracies from variations in the position of the optimum focal distance with and without the waveguide and from measuring the length of the waveguide. Such errors are constant with wavelength and can lead to the observed effective "dc offset" of the group index relative to the simulated curves. However,

#68155 - $15.00 USD Received 17 February 2006; revised 28 April 2006; accepted 1 May 2006

since this offset is constant with wavelength, it does not affect the measurement of GVD which involves taking a derivative of the group index with respect to wavelength. Still, the observed offset is small; only a 4% discrepancy from the simulated values.

Figure 3(b) shows the inferred GVD as a function of wavelength for the four waveguides. The experimental GVD is calculated by fitting the group index data to a third order polynomial and differentiating the result [11]. There is no exact functional form for the group index of a rectangular waveguide, therefore we fit our results to a third-order polynomial as an approximation over our data range. Fitting to this third-order polynomial takes into account not only GVD, but also higher-order dispersion contributions up to fourth order. As would be expected, this approximation will breakdown near the wavelength edges of our measurement, leading to the observed disagreement. Nevertheless, the variation in magnitude of anomalous-GVD and position of the zero-GVD point with waveguide cross-section clearly follow the theoretically predicted trends.

At wavelengths near 1.55 μm, the measured GVD ranges from about 200 ps/(nm·km) in the largest waveguide (300 x 650 nm), up to 1100 ps/(nm·km) in the smallest waveguide (300 x 500 nm), in agreement with the simulated GVD plotted in Fig. 3(b). This anomalous-GVD value is two orders of magnitude larger than SMF-28 fiber and one order of magnitude larger than commercially available microstructured fibers [17 ps/(nm·km) and ~200 ps/(nm·km), respectively] [1]. As an example, the measured value of 1100 ps/(nm·km) yields a dispersion length of 18 cm for a 0.5-ps propagating pulse. For the GVD to be neglected in pulse propagation, the dispersion length must be much greater than the propagation length [9]. Since the calculated dispersion length is on the order of centimeters, one would expect the GVD to significantly influence the propagation of sub-picosecond pulses in cm-long SOI waveguides. For longer pulses, GVD will not influence pulse propagation, but will determine the phase matching for nonlinear processes such as four-wave mixing [9].

5. Conclusion

In this paper we experimentally measure and numerically study the tailoring of the GVD in silicon waveguides from strongly normal- to strongly anomalous-GVD values over a wide bandwidth. We achieve anomalous values as high as 1100 ps/(nm·km) at the telecommunications wavelength of 1.55 μm. We also determine the range of sizes of silicon waveguides that allow for anomalous-GVD and investigate the effects of waveguide cross-sectional shape and size on the resulting GVD through numerical simulations. This method of tailoring the GVD in a silicon waveguide can be used to customize the GVD profile for various applications requiring such regulation. The ability to demonstrate anomalous-GVD over broad bandwidths in standard silicon waveguides enables applications such as dispersion compensation and in nonlinear optics on-chip such as four-wave mixing [23], parametric oscillation, pulse compression and soliton communications.

Acknowledgments

This work was supported by the NSF through the Center for Nanoscale Systems under award number EEC-0117770. A.C.T. also acknowledges support under a National Science Foundation Graduate Research Fellowship. M.A.F., J.E.S., and A.L.G. also acknowledge support under the DARPA Slow-Light Program. This work was performed in part at the Cornell NanoScale Facility, a member of the National Nanotechnology Infrastructure Network, which is supported by the National Science Foundation (Grant ECS 03-35765).

#68155 - $15.00 USD Received 17 February 2006; revised 28 April 2006; accepted 1 May 2006